

# RAPPORT

09 1994



NVE  
NORGES VASSDRAGS-  
OG ENERGIVERK

*Ole Einar Tveito  
Hege Hisdal*

## A STUDY OF REGIONAL TRENDS IN ANNUAL AND SEASONAL PRECIPITATION AND RUNOFF SERIES

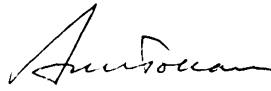


HYDROLOGISK AVDELING

Omslagsbilde: Tegnekontoret v/ Gunnlaug Moen



NVE  
NORGES VASSDRAGS-  
OG ENERGIVERK

<b>TITTEL</b> A study of regional trends in annual and seasonal precipitation and runoff series.	<b>RAPPORT</b> 09 94
SAKSBEHANDLERE Ole Einar Tveito Hege Hisdal	DATO 10.03.94
	RAPPORTEN ER åpen
OPPDRAGSGIVER Norges Forskningsråd/Norsk Hydrologisk Komite	OPPLAG 50
<b>SAMMENDRAG</b> I denne undersøkelsen er lange og homogene tidsserier for avløp og nedbør studert for å identifisere variasjoner i tid og rom. Til dette er empiriske ortogonale funksjoner (EOF-metoden) benyttet. Både årlige, glattede (ved bruk av Gauss-filter) og sesongverdier er undersøkt. Analysen viser at de årlige variasjonene i nedbør og avløp er sammenfallende. Avvik som opptrer for sesongverdier er forårsaket av snøakkumulering og snøsmelting. I de filtrerte seriene gjenspeiles trender. For nedbør er en sammenligning mellom de forskjellige normalperiodene utført. Denne viser at periodene 1900-30 og 1960-90 oppfører seg forskjellig fra perioden 1930-60. Dette kan skyldes at ulike værtyper har dominert i de enkelte periodene. Forskjellige værtyper reflekteres i ulike empiriske ortogonale funksjoner. Dette bekreftes gjennom regionale studier. At nedbør og avløp følger samme mønster er et viktig resultat med tanke på klimastudier og ekstrapolasjon.	
<b>ABSTRACT</b> In this study long and homogeneous time series of runoff and precipitation are studied to identify variations in time and space. The method of empirical orthogonal functions (EOF-method) is applied. Both annual observations, smoothed (using Gauss-filter) and seasonal values are analyzed. The analysis shows that the temporal variations in runoff and precipitation coincide. The deviations occurring in the seasonal values are caused by snow accumulation and snow melt. In the filtered series temporal trends are found. A comparison between the different normal periods has been carried out for precipitation. The 1900-30 and 1960-90 periods differ from the 1930-60 period. This may be caused by different weather types dominating in the different periods. The different weather types are reflected in different empirical orthogonal functions. This is verified by regional studies. The coinciding patterns in runoff and precipitation are important aspects in climate studies and for extrapolation purposes.	
EMNEORD/SUBJECT TERMS empiriske ortogonale funksjoner/empirical orthogonal functions klimaendringer/climate change regionale trender/regional trends avløp/runoff nedbør/precipitation	ANSVARLIG UNDERSKRIFT  Arne Tollan Avdelingsdirektør

## PREFACE

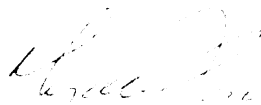
To determine the local response of a possible climate change, regional trends in runoff and precipitation have to be mapped. It is also important to find the response and contribution of different weather systems in runoff and precipitation series.

In this study the method of empirical orthogonal functions (EOF-method) has been used to separate variations in time and space. The application of the EOF-method used on yearly, seasonal and Gauss-filtered runoff and precipitation series is described. A presentation of the results, and the connection between the results and physical processes is given.

The study is carried out at the Norwegian Water Resources and Energy Administration (NVE) in cooperation with The Norwegian Meteorological Institute (DNMI) and the Department of Geophysics at the University of Oslo (UiO). The authors would especially like to thank Eirik Førland and Inger Hanssen-Bauer at DNMI for providing a large data set and giving constructive comments on the analysis and results. We would also like to thank professor Lars Gottschalk at UiO and professor Nils Roar Sælthun (NVE/UiO) for advices and valuable comments throughout this work.

The project was financially supported by the Norwegian Research Council.

Oslo, March 1994



Kjell Repp  
Section manager

## Content.

	page
1. Introduction	4
2. Review of methods	5
2.1 EOF-method	5
2.2 Rule N	5
2.3 Gauss filter	6
3. Data sample	8
4. Analysis	10
4.1 Application of the Rule N method on precipitation and runoff series	10
4.2 Annual series	10
4.2.1 Unfiltered series	10
4.2.2 Filtered series	14
4.3 Precipitation 1900-90	18
4.4 Seasonal values	18
4.5 Periodical studies	23
5. Regional estimates	25
6. Conclusions	29
References	30

## 1. Introduction

One problem concerning *climate change* is to separate changes due to human activities from the natural variability. Studies of long and homogeneous climatic time series are important in this context. In previous studies (Førland et.al. 1991, Førland and Hanssen-Bauer 1992, Roald and Sælthun 1990) time fluctuations in precipitation and runoff were analysed. These investigations show systematic regional differences in runoff and precipitation. Still, no comparative study of runoff and precipitation has been carried out.

The method of empirical orthogonal functions (the EOF-method) is suitable for separating temporal and spatial variations in time series. In Norway the method has been used for extrapolation (Hisdal and Tveito, 1993), spatial interpolation (Hisdal and Tveito, 1992) and regionalization of runoff series (Hisdal and Tveito, 1990). In these studies no attempts have been made to isolate temporal trends.

Lins (1985) compared principal components of runoff, precipitation and a drought index for the United States to find relations between runoff and meteorological variables. He found remarkable coincidence between the variables. Pandžić and Trninić (1991) made a study in the Kupa basin in Croatia, to find the annual pattern of runoff in terms of principal components of precipitation and water balance. Both studies found principal components suitable for such analysis and application.

In this investigation long precipitation and runoff series are analysed applying the method of empirical orthogonal functions. The results from the EOF-analysis are used to identify the variations in time of the major components of the series. Regional differences in the components are evaluated studying the spatial variation of the weight coefficients from the EOF-analysis. The analysis was carried out for several data sets, using different periods, gauss-filters of varying lengths and different seasons. A comparison of the three 30-year normal periods of this century has been carried out. The objective of this analysis has been to get a better understanding of the regional variations in precipitation and runoff. The EOF-method has been used for decomposition of the variations to explain them by climatic characteristics.

The study has been carried out at the Norwegian Water Resources and Energy Administration, with valuable support and cooperation from Department of Geophysics, University of Oslo (computer resources and scientific discussions) and Department of Climate, Norwegian Meteorological Institute (precipitation data series and scientific discussions).

## **2. Review of methods**

### 2.1 The EOF-method

The method of empirical orthogonal functions has been applied for several purposes within the hydrosociences during the last three decades. This method has showed to manage large sets of spatial and temporal data in an efficient way.

For a detailed description of the method see Essenwanger (1976). In the following a short presentation is given to explain the utilization in this study.

The principle behind the method is a linear transformation of a set of correlated spatially distributed time series (in this study runoff and precipitation series) into two new sets of orthogonal and thus uncorrelated functions. This transformation can be described as:

$$X(u,t) = \sum_{j=1}^N h_j(u)\beta_j(t)$$

where:

$\beta_j(t)$  are amplitude functions.  
 $h_j(u)$  are weight coefficients.

The amplitude functions contain the temporal variations of the original time series. A few of these functions will contain most of the variation in the original series. They are arranged in descending order according to the proportion of variance explained by each function. Consequently, most of the variation will be explained by a few functions. Redundant information in the lower ranked amplitude functions can be removed.

The weight coefficients describe the contribution of the amplitude functions to the original series. These weights can be regarded as the spatial component of the process  $X(u,t)$ .

### 2.2 Rule N

To examine the number of significant amplitude functions, the Rule N significance test was used. The method is explained in detail by Preissendorfer (1988). Only a short description is given here.

The method is based on a Monte Carlo simulation giving samples with distribution  $N_p(\mathbf{0},\mathbf{1})$ . The null hypothesis is that a  $n \times p$  data matrix  $\mathbf{Z}$  is drawn from such a population.

A Monte Carlo simulation gives 100 independent  $n \times p$  samples. For each sample the eigenvalue  $\ell_j$  is calculated. The eigenvalues are arranged as follows:

$$\ell_j(\omega) > \dots > \ell_\rho(\omega),$$

where  $\rho = \min[n-1, p]$  and  $\omega = 1, \dots, 100$ . Then  $U_j(\omega)$  is calculated:

$$U_j(\omega) = \ell_j(\omega) \left[ \rho^{-1} \sum_{k=1}^{\rho} \ell_k(\omega) \right]^{-1}$$

$U_j(\omega)$  is ordered for each  $j$ :

$$U_j(\omega_1) < \dots < U_j(\omega_{100})$$

$\rho_j(05) \equiv U_j(\omega_5)$  and  $\rho_j(95) \equiv U_j(\omega_{95})$ . These two values define the 5% and 95% points on the cumulative distribution of the  $j$ 'th eigenvalue. Similarly for the real data set  $\mathbf{Z}$  the eigenvalues are arranged  $d_1 > \dots > d_\rho$  and:

$$V_j = d_j \left[ \rho^{-1} \sum_{k=1}^{\rho} d_k \right]^{-1}$$

In both cases  $j=1, \dots, \rho$  and  $\omega=1, \dots, 100$ .

The *Rule N* says that the significant number of amplitude functions  $p'$  is:

- $p'$  is the greatest  $j$  for which  $V_j > \rho_j(95)$
- $p'$  is zero if no such  $j$  exists.

The Rule N can easily be visualized by plotting the  $V_j$ ,  $\rho_j(05)$  and  $\rho_j(95)$ . When the  $V_j$ -line crosses the  $\rho_j(95)$ -line, the amplitude functions do not significantly contribute to explain the process.

### 2.3 Gauss filter

To identify long time trends in the data series, a Gauss filter was applied. Using filtered values, single values are suppressed in favour of a value representative for the filter length. This filter was selected because it gives a better consistence between observed and filtered extreme values than the more traditional moving average filter. The Gauss filter is a weighted model, giving the central years the most significant weights. The weights are given by:

$$w_{ij} = e^{-\frac{(i-j)^2}{2\sigma^2}}$$

where  $i$  and  $j$  are indexes in time and  $\sigma$  the standard deviation. The filtered value is given by:



$$G_j = \frac{\sum_{i=1}^n w_{ij} x_i}{\sum w_{ij}}$$

where  $\sigma$  is the standard deviation and  $x_i$  is the observed value. The filter length depends on the standard deviation chosen. The tails of the time series are filtered to one side only, and therefore less reliable than the filtered values in the middle of the series. One should therefore be careful in interpreting trends in the beginning and end of the filtered time series.

### 3. Data sample

The investigation requires long and homogeneous time series. To be able to do the EOF-analysis, missing values are not allowed within the period to be examined. For this investigation 129 precipitation series was available. These are either homogeneous or corrected for heterogeneity (Førland et.al., 1991).

The runoff series are to represent natural runoff. This means that the series should be selected from unregulated catchments or adjusted for regulations. A short study examining the homogeneity of runoff series (Aagenæs, 1993) resulted in 68 series available for this analysis, fulfilling all our requirements.

The locations of the data series are shown in figure 3.1. The data series consist of monthly values. Due to the demand of complete series, the number of series included in the analysis varies, depending on the period studied.



Figure 3.1 Location of the data series used in the analysis. Runoff series are marked as asterisks, precipitation series with a stand.

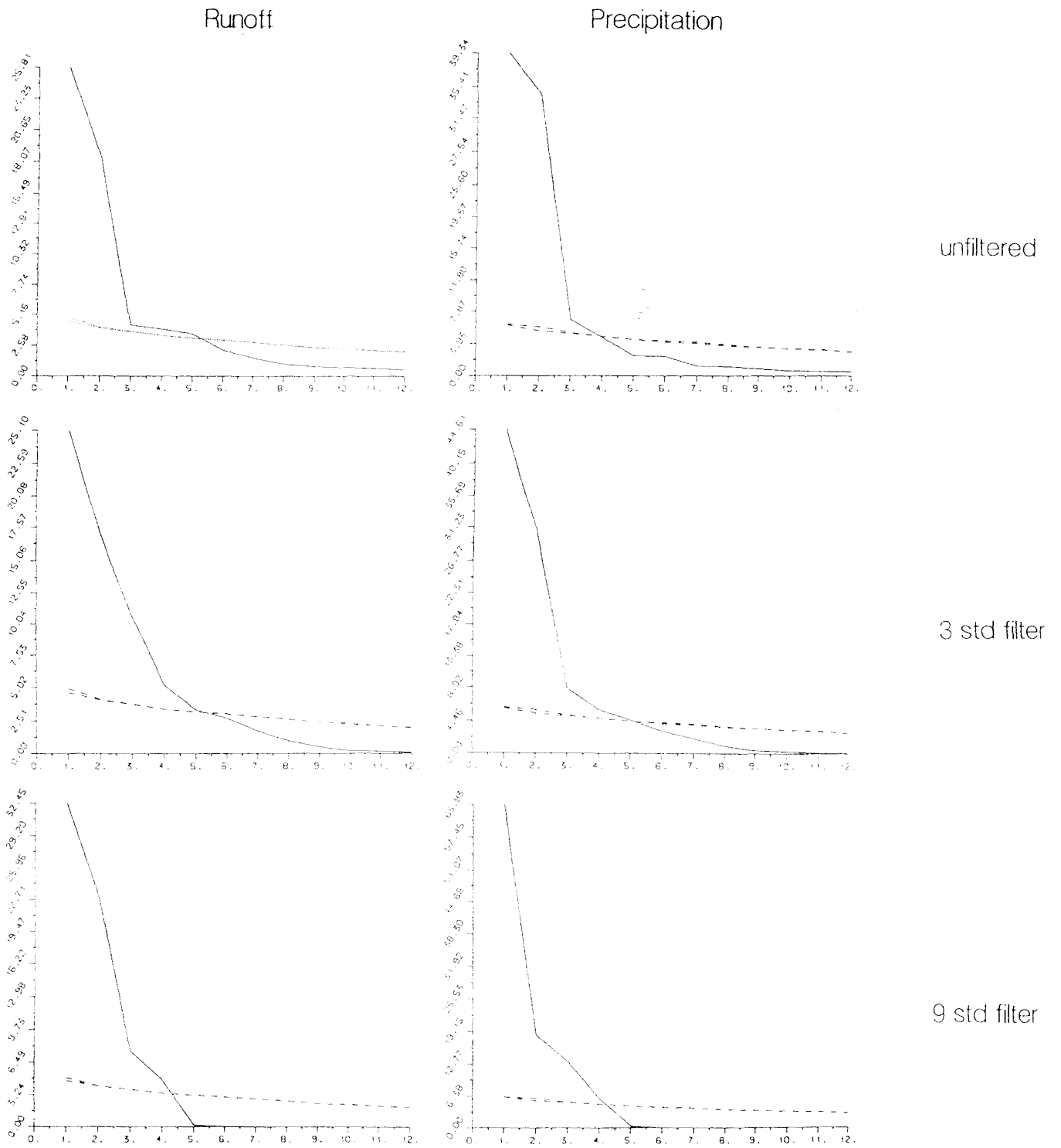


Figure 4.1 Rule N applied on the different data sets in this analysis. The ordinate shows the eigenvalue and the abscissa the number of amplitude functions. The eigenvalues of the data sets are plotted as a solid line, the eigenvalues of  $\rho(05)$  and  $\rho(95)$  of the random reference sets with dashed lines.

## **4. Analysis**

Both annual and seasonal series are analysed. Standardized and Gauss-filtered runoff and precipitation were studied. In each case an EOF-transformation produced weight coefficients and amplitude functions. The weight coefficients were analysed using contour maps and scatterplots, and the amplitude functions by plotting them as time series. Contour maps show the spatial variation of the weight coefficient. In the scatterplots regional grouping based on the two weight coefficients plotted can be discovered. The behaviour of the amplitude functions is used to detect temporal trends in the material.

### 4.1 Application of the Rule N method on precipitation and runoff data

The Rule N test was applied on all the data sets of annual values of precipitation and runoff, unfiltered and filtered, used in this study. The results were plotted, showing that the significant number of amplitude functions varies from three to five (figure 4.1). In this study only the first three components are considered. The number of significant amplitude functions is higher for runoff series than for precipitation series. This difference is a result of the larger variability of the runoff data caused by catchment processes.

The relative contribution of the components can be seen from the plots.

### 4.2 Annual series

Annual series from the period 1930-90 was analysed both for runoff (68 series) and precipitation (102 series), separate and together.

#### 4.2.1 Unfiltered series

The first three amplitude functions of runoff and precipitation are shown in figure 4.2. They contain 71 and 79% of the variance of the original runoff and precipitation series respectively. The functions of runoff and precipitation are almost similar. The annual series of the two variables have the same temporal variations. From the plots it is not possible to identify trends in the data set.

In the analysis calendar years are used. This may cause some problems comparing runoff and precipitation. Autumn precipitation as snow is not reflected in the runoff until the next year. If the amount of precipitation stored as snow is large a delay between precipitation and runoff amplitude functions may occur.

To map the regional differences, the weight coefficients have to be examined. Contour plots illustrate the spatial variability of the weight coefficients. The first coefficient of runoff (figure 4.3a)

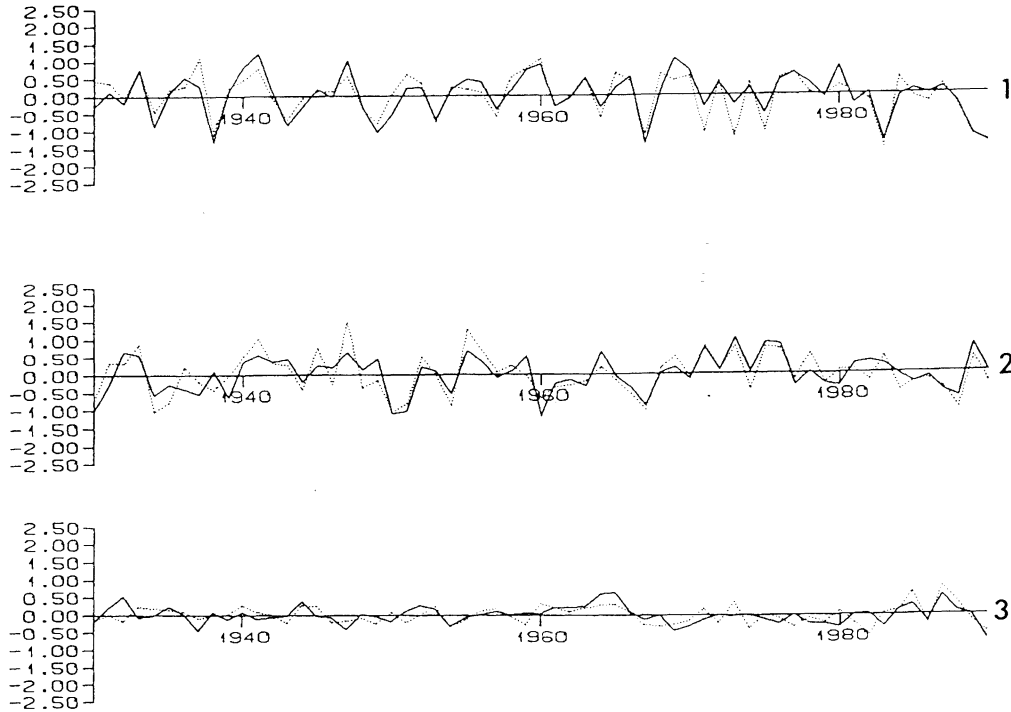


Figure 4.2 The first three amplitude functions for the period 1930-90, yearly values. The solid line represents runoff, the dashed line represents precipitation.

has a smooth variability. An east-west change in the coefficient is recognized in southern Norway. In northern Norway the change is northwards. The second component has an even more regular behaviour. The pattern is somewhat rotated compared to the first component, the slope has a northwest/southeast gradient. The third coefficient is orientated east-west.

The contour plots of the precipitation coefficients are even more regular than for runoff. The first coefficient is shown in figure 4.3b. Its gradient is a little rotated towards west-northwest compared to runoff. The second coefficient contours are almost identical with the runoff pattern. The third is a little rotated west-southwest compared to runoff.

For regionalization, scatterplots are convenient. Figure 4.4a shows a scatterplot of the first weight coefficient for runoff plotted against the second. Clear groups are seen in the figure. It confirms that the first coefficient explains an east-west, or a coastal/continental relation. The second coefficient seems to catch variation in the north-south gradient. Five distinct groups can be recognized. The glacier catchments fall outside these groups. The geographical positions of the groups are shown in figure 4.4b. The first and third coefficient give a scatter from wet to dry areas. The

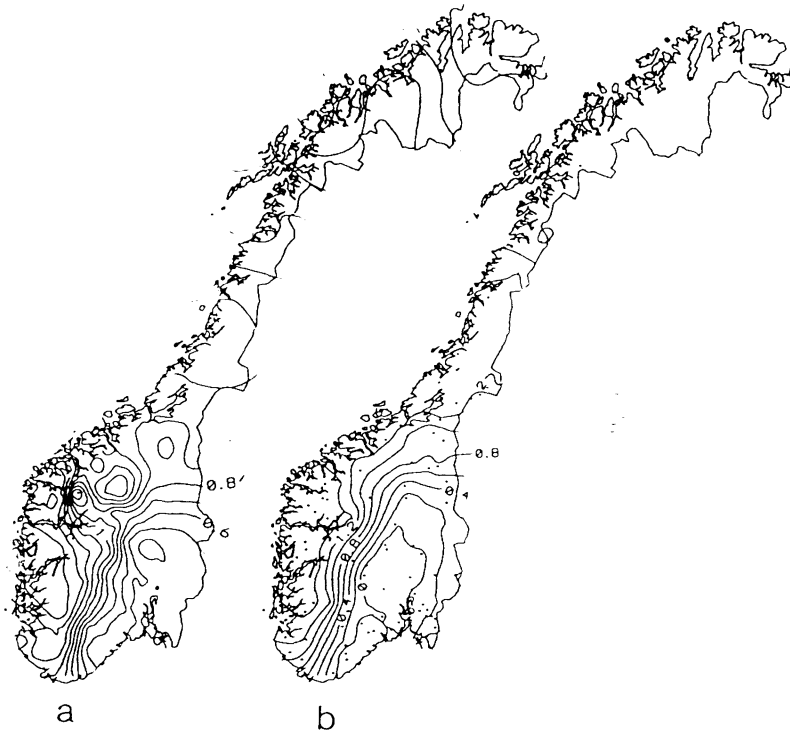


Figure 4.3 Contour plot the first weight coefficient yearly values 1930-90:  
a) Runoff.  
b) Precipitation.

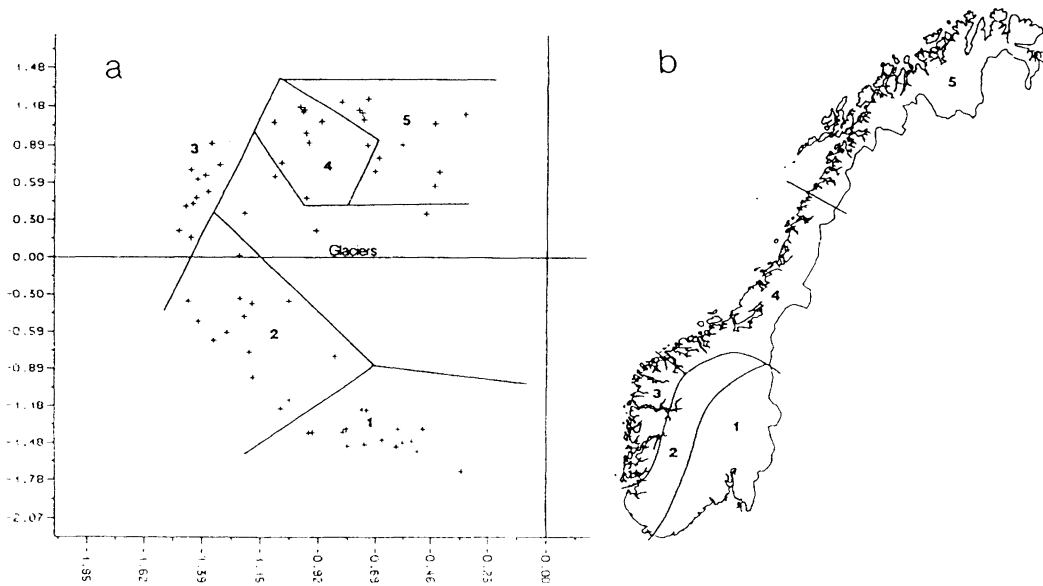


Figure 4.4 Regional grouping based on the first two weight coefficients of runoff.  
a) Scatterplot.  
b) Resulting regions.

second and third coefficient show an almost circular distribution, starting in north following the coast anticlockwise ending in the inner parts of southern Norway. From these plots it seems like the third coefficient explains dry/wet conditions.

The same three scatterplots were analysed for precipitation. Absence of stations in Troms and Finnmark gives one missing group in the first versus the second weight coefficient. There are some minor differences between runoff and precipitation. This is caused by different spatial distribution of input series to the EOF-analysis. The plots of the first coefficient versus the third and the second versus the third gave the same pattern as for runoff.

The EOF-analysis shows that the main temporal and spatial patterns of annual runoff and precipitation are equal. Consequently, the two data sets were combined and analysed. The contour plots are shown in figure 4.5. As for the individual studies of runoff and precipitation, the different components have different geographical orientations. The first component has an east-west gradient, which implies that this component is caused by westerly weather systems. The other two components are results of northwesterly respectively west-southwesterly weather systems. The conditions are probably controlled by dominating wind directions. This should be further examined by including dominating pressure fields to the analysis, but is not within the frame of this investigation.

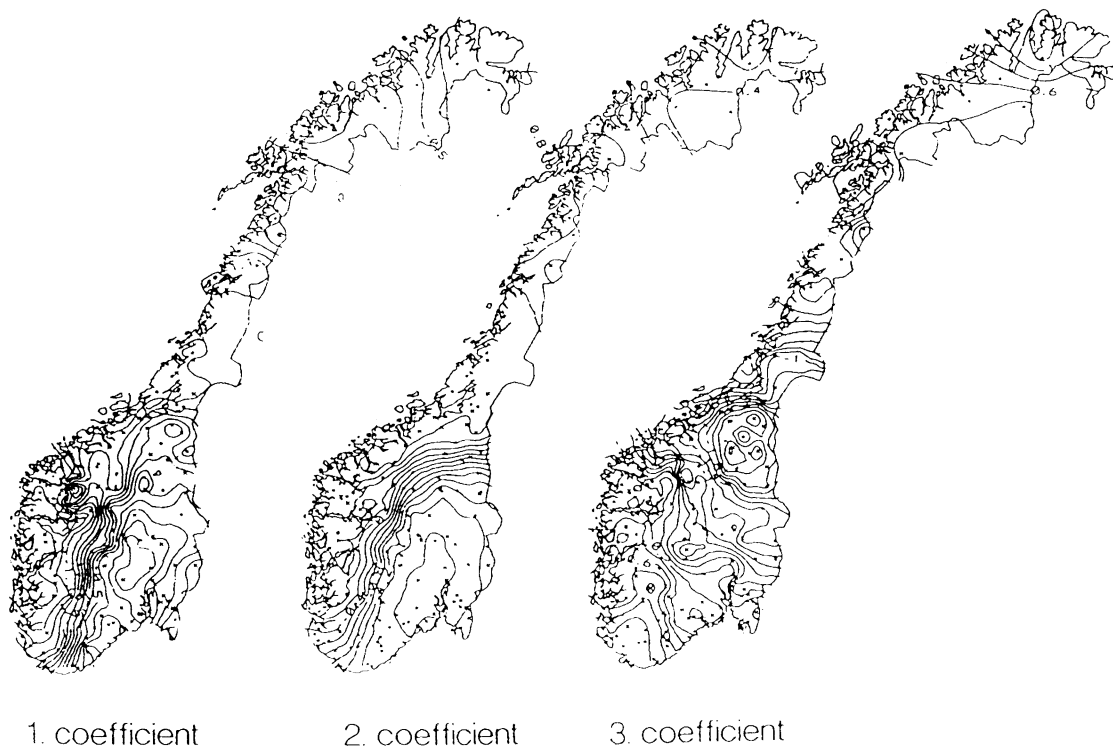


Figure 4.5 Contour plots of the first three weight coefficients of the combined data set.

#### 4.2.2 Filtered series

Filtered series of runoff (1930-90) and precipitation (1900-1990) are established. Two filter lengths are used, 3 and 9 standard deviations. This gives filters of 28 and 55 years respectively.

The period 1930-90, filter length 9 standard deviations.

The amplitude functions resulting from the EOF-analysis of the  $9\sigma$  (filter length 9 standard deviations) are shown in figure 4.6. Long term fluctuations are reflected in the functions. The number of fluctuations seems to increase with increasing number of the function. The first three functions explain 93% of the original variance. The following properties are seen:

- The gradient of the first function is increasing from around 1960.
- The second function turns around 1970.
- The third function seems periodic.

The same pattern as for the runoff functions is recognized for precipitation.

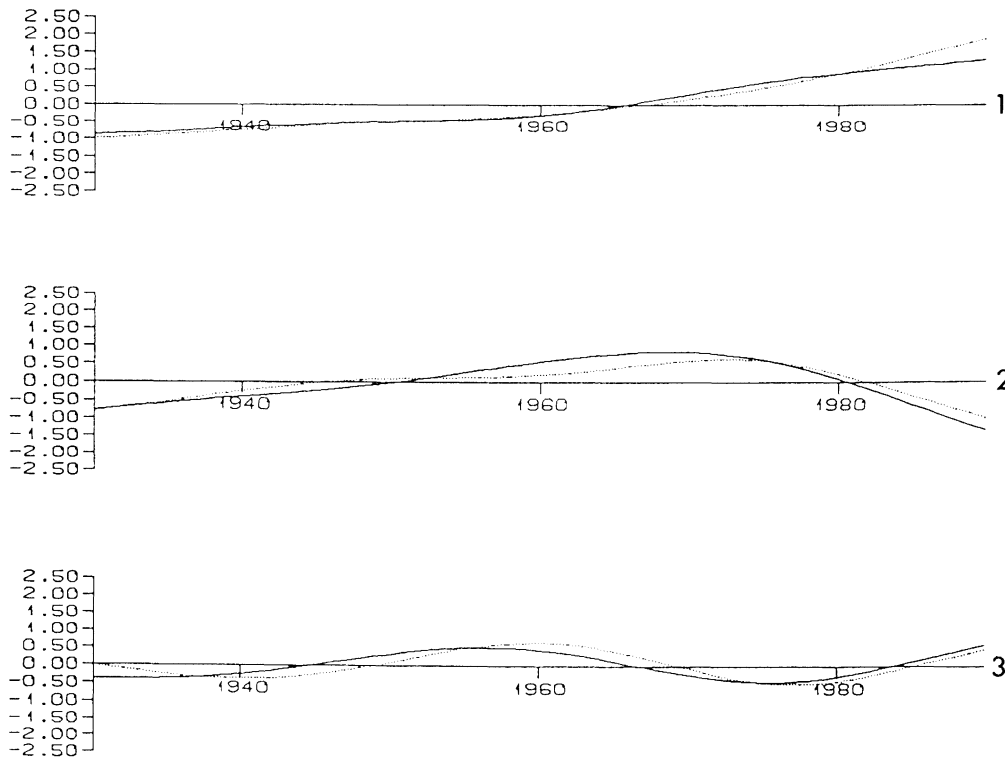


Figure 4.6 The first three amplitude functions for the series filtered with a  $9\sigma$ -filter. Period 1930-90. Runoff is represented by a solid line, precipitation with a dashed line.



We cannot assume that the same properties are represented in the amplitude functions of the filtered series as in those of the unfiltered series. The filtered series have other statistical properties than the original series, and therefore the expansions into EOFs will differ. Generally one should be careful to interpret the physical meaning of the amplitude functions, since they solely reflect statistical properties.

The contour map of the first coefficient of runoff is shown in figure 4.7a. Compared to the map of the unfiltered series (fig. 4.4) this map contains more variability. The filtered series are smoothed, and fluctuations from the general regional patterns may therefore give large deviations in the magnitude of the weight coefficients. This is seen in figure 4.7a where stations deviating from the regional behaviour, cause sharp circles in the contour map (e.g., in the glacier area in the northwestern parts of southern Norway). This shows that the glacier catchments have different long term climatic characteristics compared to catchments not covered by glaciers, due to long response period of precipitation input.

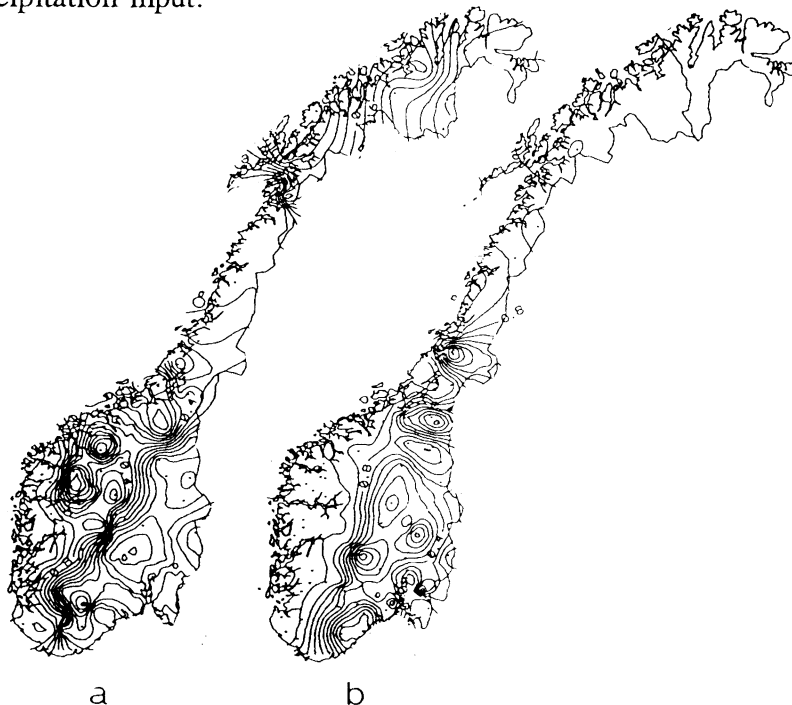


Figure 4.7 Contour map of the weight coefficients for the  $9\sigma$ -filtered series.  
a) Runoff.  
b) Precipitation.

The main gradient of the first weight coefficient is northwesterly in southern Norway and westerly in northern Norway. In Nordland the lack of series cause that no trustworthy contour lines can be established. The major patterns are the same as for unfiltered series, but the patterns of the filtered series are a little rotated to northwest. There are also some differences in the northern parts of Eastern Norway.

The magnitude of the second weight coefficient of runoff changes from east to west. Some variability in the high mountain and glacier areas in southern Norway occurs.

The third weight coefficient changes in a southwesterly gradient. In this coefficient, strong local variability is found in the glacier and high mountain areas. These patterns differ from those found in the unfiltered series.

When examining the contour plot of the first weight coefficient for precipitation (figure 4.7b), an almost east-west gradient is seen. The values at the west coast are remarkable-stable, implying that the influence of the first amplitude function is the same for the whole area. The variations east of the mountains are mainly controlled by single observations deviating from the regional mean. An exception is the south-coast (Agder), which shows a significant variation from the surrounding areas. In Trøndelag local variations are present. In this area the natural variability is large, and the conditions are highly dependent of the dominating wind direction. It is therefore sensitive to changes in the wind direction. Due to few stations in the northern parts of Norway, the results here are not interpreted further.

For precipitation the second weight coefficient has dominating southwest-northeast gradient. The Agder area differs from the general pattern. It is seen that the values at the west-coast are stable. The eastern parts, north of the Oslofjord, also can be considered as an area with stable values. Some local, partly large, variations do though occur at certain stations. Still, three regions can be established.

The third coefficient contour map of precipitation shows a wet-dry component with stable values at the west coast. East of the mountains there is a strong gradient. In Trøndelag there is some local, but smooth variations.

As for the unfiltered series of runoff and precipitation, the grouping of the weight coefficients is examined studying scatterplots. It is difficult to establish clear groups from the scatter plots. Some tendencies are found, but the general impression is chaotic. Since the filtered series are smoothed series, the variance of the series is small. This will be reflected in the EOF-analysis, giving large variations in weight coefficients for deviating series.

From the study of the three coefficients, it is possible to isolate some regions where the weight coefficient values are stable. When an area is considered to have stable values, the whole area is reacting almost equally to the different components developed by the EOF-analysis. The values for all coefficients are remarkable stable at the west coast. Also, the Agder area is stable. Eastern Norway has the same characteristics, but in this area large local variations occur. The east side of the Oslofjord (Østfold) shows stable values for all three coefficients. This is interesting, since there are no runoff series available from this area.

The period 1930-90, filter length 3 standard deviations.

The analysis of the series resulted filtered with a 3 standard deviation filter length showed the following results:

The three first amplitude functions (figure 4.8) are periodic with periods of about 10 years. The first function has the most regular fluctuations, except in the first and last part of the period. These irregularities can be a result of the mirror effect. The functions for runoff and precipitation are with a few exceptions equal.

The second and third functions also have fluctuations, but with more irregular amplitudes. This indicates that the first function contains the general conditions common to the whole area during the period, while the more regional information is found in the lower ranked functions. A further investigation of the spatial behaviour of the weight coefficients confirms this.

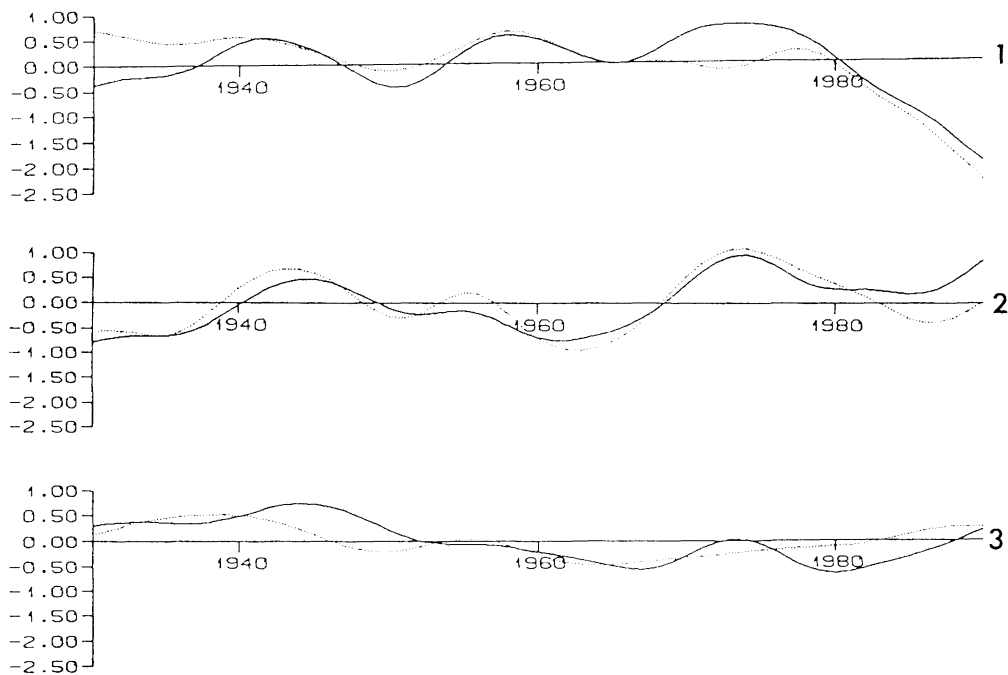


Figure 4.8 The first three amplitude functions for the series filtered with a  $3\sigma$ -filter. Period 1930-90. Runoff is represented by a solid line, precipitation with a dashed line.

An examination of the weight coefficient scatter plot for runoff shows regional tendencies in the first two coefficients, resulting in three groups. The first coefficient shows a south-north variation, while the second has an east-west change. The third coefficient lacks clear regional variation. A study of the contour plots confirms this impression.

Studying the contour plots for precipitation, a weak east west relationship is seen in the first weight coefficient. The second coefficient shows a smooth variation, with an east west gradient. The third coefficient plot is chaotic with no marked directions. Scatterplots confirm the impression found in the contour plot.

It is interesting to see the difference in the first weight coefficient of precipitation compared to runoff. The runoff coefficient pattern is chaotic compared to the smooth variations in the precipitation coefficients. This can be an effect of both catchment processes and the spatial distribution of input series.

### 4.3 Precipitation 1900-1990

78 of the precipitation series cover the period 1900-1990. These series, filtered as well as unfiltered, are used as input to an EOF-analysis.

The amplitude functions have the same fluctuations as for the period 1930-90. The amplitudes might be a little different due to other statistical properties of the reduced data sample. The most remarkable characteristic of the first amplitude function is the period of almost constant value from ~1930 - 1955. In the series of 1930-90 this period shows a weak decreasing tendency.

Contour and scatterplots were examined to find regional characteristics of the precipitation. The contour plot of the first weight coefficient shows little difference from the plots of the period 1930-90. The scatterplot of the first vs. the second weight coefficient of the filtered series with  $3\sigma$  shows little variation in the first weight coefficient. The second coefficient shows more variation. In the scatterplot a wet-dry (southeast-northwest) gradient is indicated, and this is confirmed by the contourplot. The third coefficient also shows a wet-dry gradient, but rotated towards southwest-northeast.

The study of the  $9\sigma$  filter analysis gave the following characteristics: The scatter shows more variation in the first coefficient than for the  $3\sigma$  example. Examining the first vs. the second weight coefficient, it is possible to isolate some groups. In the contour plot of the first coefficient (figure 4.9) the Agder region is clear, but also an inland region north and west of Oslo is recognized. The second coefficient contourplot also gives a further regionalization in a western, an eastern and a northern region as shown in figure 4.10. The third coefficient shows an east-west orientation with considerable "noise."

### 4.4 Seasonal values

An analysis on seasonal mean values was carried out. Only unfiltered series were used. The seasons defined are winter (December-February), spring (March-May), summer (June-August) and autumn (September-November). Only the contour plots are studied.



Figure 4.9 First weight coefficient contours for precipitation for the period 1900-90,  $9\sigma$ -filter.

Figure 4.10 Second weight coefficient contours for precipitation for the period 1900-90,  $9\sigma$ -filter.



Figure 4.11 First weight coefficient contour plots of seasonal values of precipitation. a) winter, b) spring, c) summer and d) autumn.

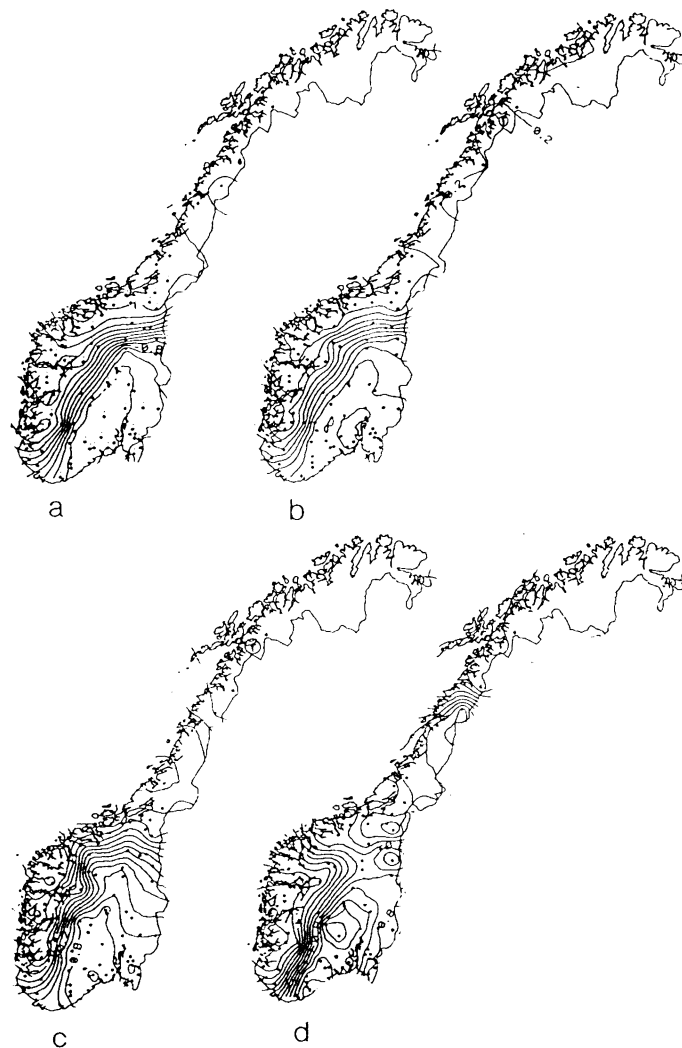


Figure 4.12 Second weight coefficient contour plots of seasonal values of precipitation. a) winter, b) spring, c) summer and d) autumn.

The spatial behaviour of the first weight of precipitation for the different seasons is shown in figure 4.11. The major patterns are the same, except in the summer season. This season is characterized by little variation in southern Norway. For the other seasons the gradient is large. If a larger area has little variation in the weight coefficients it implies that all stations have the same spatial pattern of the physical characteristics connected to the corresponding amplitude function. The variability that occurs in this area is therefore found in other amplitude functions. This is the case of the eastern parts of south Norway in the summer season. Large scale processes, like frontal systems, dominate small scale processes such as convective activity. In the summer season small scale activity dominates in southeastern Norway. However, this activity is not reflected before in the third amplitude function.

When it comes to the second coefficient (figure 4.12), the autumn season differs from the others. The Trøndelag district has the same weight coefficient value as for the eastern parts of south Norway instead of following the coastal influence. There are only small variations between the seasons for the third coefficient.

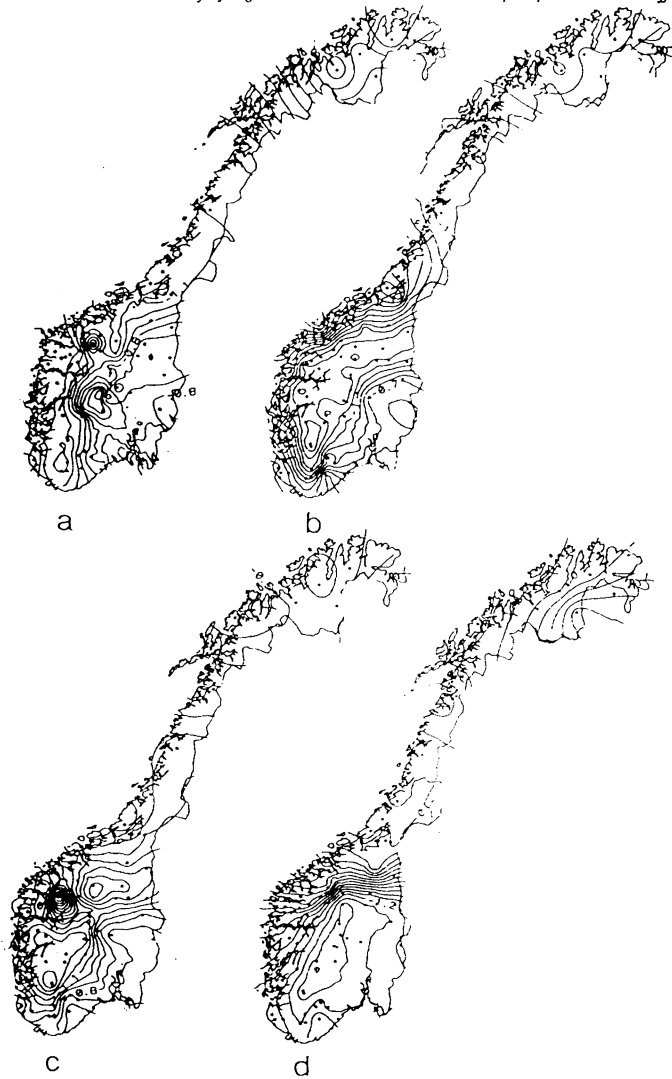


Figure 4.13 First weight coefficient contours of seasonal values of runoff. a) winter, b) spring, c) summer and d) autumn.

The contour plots for the first weight coefficients of runoff for the four seasons are shown in figure 4.13. The winter season has the same pattern as for precipitation, but large local deviations are present. In the spring season the weight coefficient pattern differs a lot from the precipitation coefficient pattern. This season has a maximum zone in the mountain area, due to snow melt. In the summer period an extreme maximum is detected in the Jostedal Glacier area. In the southern parts of the country the same patterns are found in precipitation and runoff. The difference in the southeastern parts is probably caused by differences in the station network. In the autumn the runoff and precipitation pattern coincides.

The second coefficient is shown in figure 4.14. Surprisingly the general patterns for runoff and precipitation coincide for the first three seasons. This means that the snow melt is not reflected by the second amplitude function. The autumn is also very similar, but there are some differences in the Møre area and northwards.

The third coefficient shows extreme gradients in Finnmark in the winter period. Generally the characteristics are the same for runoff and precipitation, but local variations can be large in mountain areas. The patterns for the spring period largely have the same characteristics

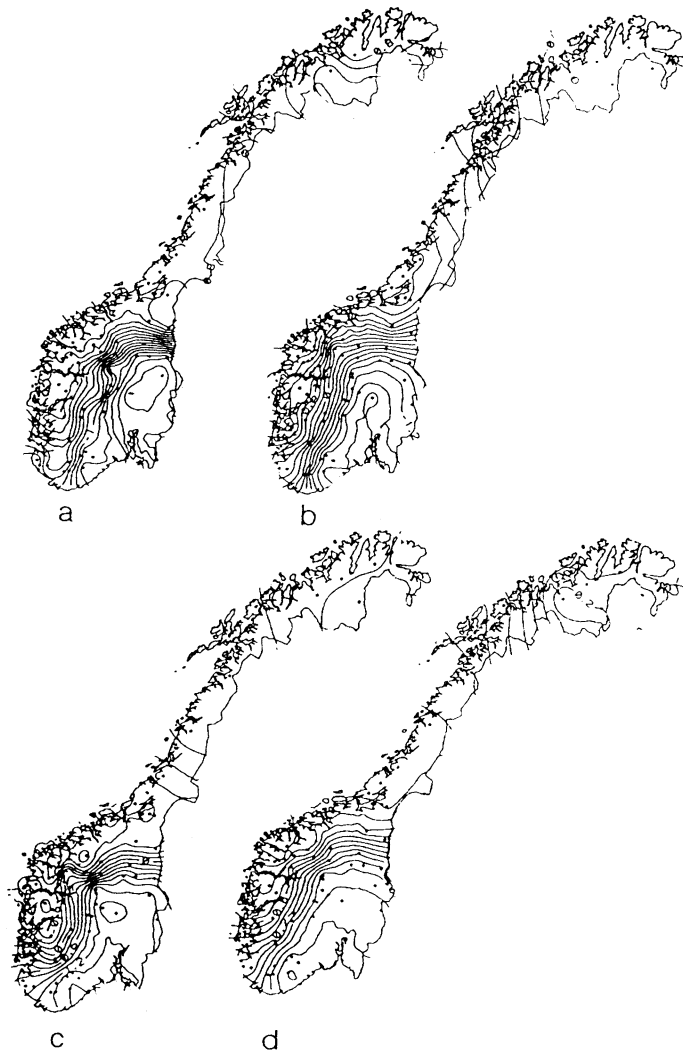


Figure 4.14 Second weight coefficient contours of seasonal values of runoff. a) winter, b) spring, c) summer and d) autumn.

as the first coefficient, and are very different from those of to precipitation. In the summer period there is a maximum in high mountain areas, probably explaining summer snow melt. The patterns deviate strongly from the behaviour of precipitation. In the autumn the contour maps for precipitation and runoff are similar.

Differences between the two variables can primarily be explained by snow melt, as expected, and probably by the varying station cover in certain areas.



#### 4.5 Periodical studies

To examine temporal changes in the physical characteristics of the principal components, the series of precipitation was divided into three sub periods of 30 years. An EOF-analysis was carried out for each period. The spatial distribution of the weight coefficients was examined.

Contour maps of the first coefficient are shown in figure 4.15. The first and last period show

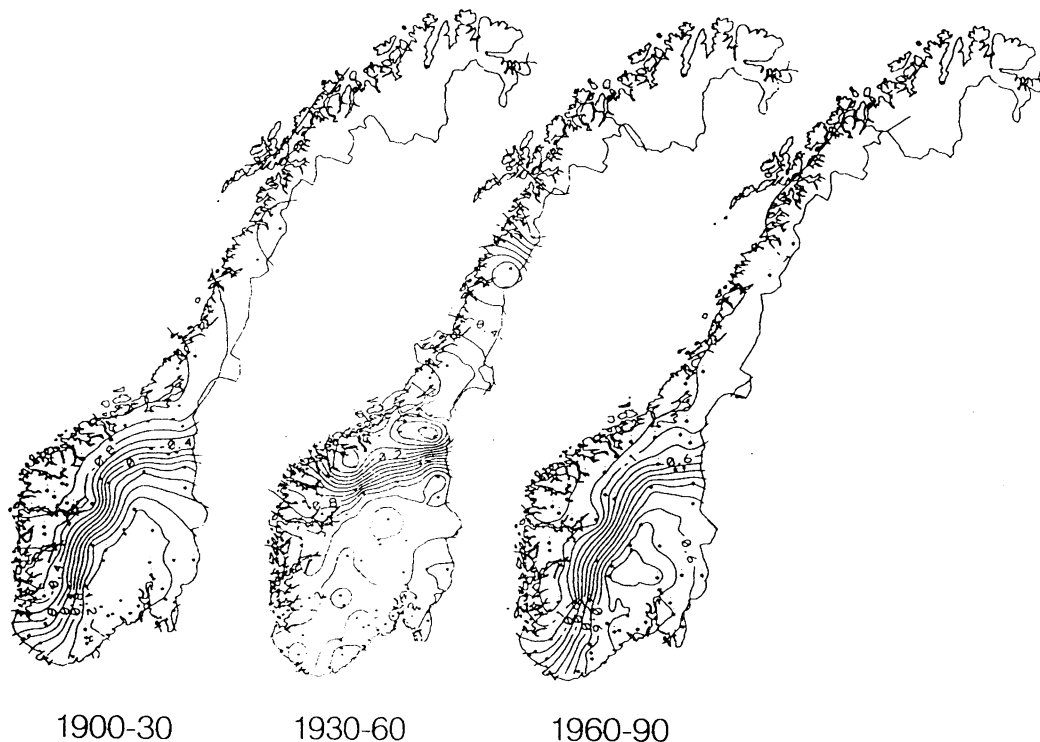


Figure 4.15 Contours of the first weight coefficient of the three normal periods in this century for precipitation,  $9\sigma$ -filter.

the same behaviour. The weight coefficient field is orientated along the mountains in southern Norway, in a west-northwest orientation. In the period between a different pattern occurs. This period has a north-northwest orientation with a strong gradient south of Trøndelag and very little variation in the southern parts. The difference coincides with the behaviour of the first amplitude function of the  $9\sigma$  filtered series described in the section 4.4 (figure 4.16). This may be caused by a change in the dominating weather directions. The pattern of the first and last period is also found in the second function of the middle period. The first function explains 42, 44 and 43% in the respective periods, the second 26, 32 and 27%. These numbers tell that the differences between the functions are small, and that a little variation in the data series can cause a "shift" between the functions.

The second coefficient (figure 4.17) shows variation in each of the three periods. The first period has a westerly orientation. The period 1930-60 shows a pattern very similar to that of the first

coefficient for the periods of 1900-30 and 1960-90. In the last period, the second coefficient has a northwestern orientation with gradually decreasing weight coefficient values.

For the third coefficient the same as for the first coefficient happens. The first and last period show similar behaviour, with a westerly gradient dominating. The second period has a southwestern orientation.

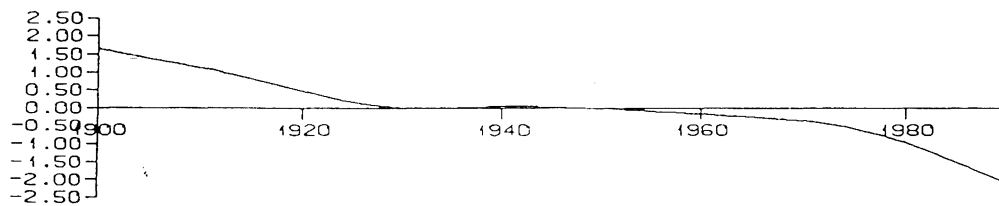


Figure 4.16 The first amplitude function of precipitation,  $9\sigma$ -filter, for the period 1900-90.

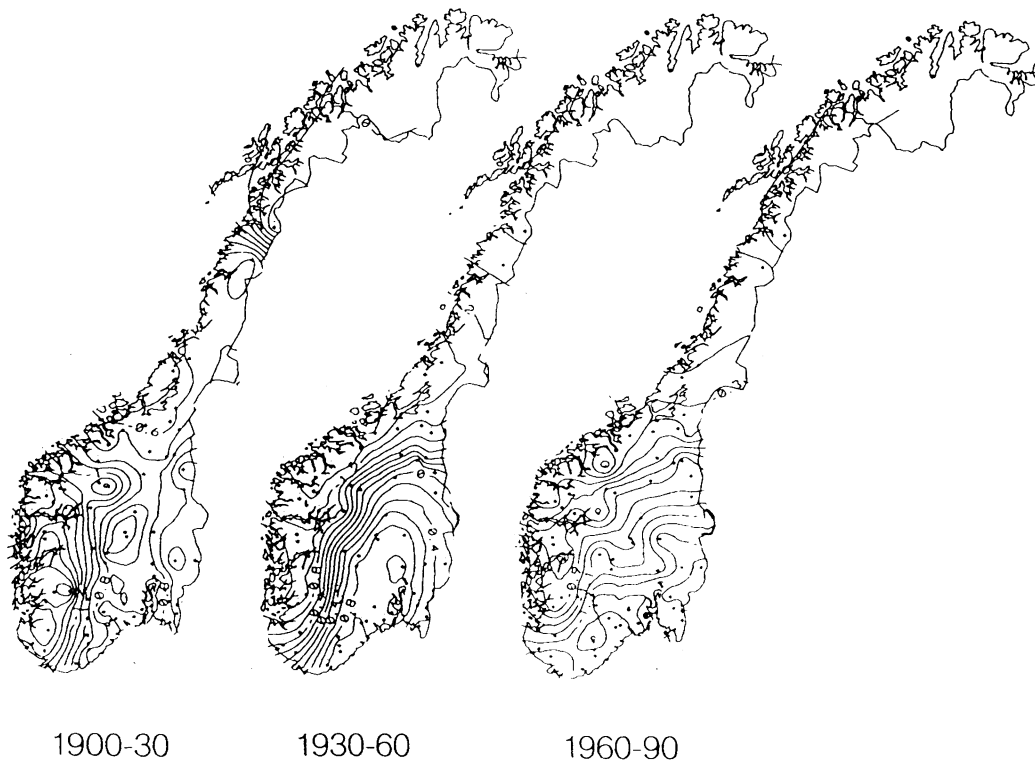


Figure 4.17 Contours of the second weight coefficient of the three normal periods in this century for precipitation,  $9\sigma$ -filter.

## 5 REGIONAL ESTIMATES

To analyse the influence of the different amplitude functions in different parts of the country, a verification analysis for several series was carried out. The observed series were plotted with both the individual contributions from the amplitude functions, and the sum of all three functions. The following expression was used:

$$x(u,t) = m(u) + s(u) \cdot \sum_{j=k}^n h_j(u) \cdot \beta_j(t)$$

where:

- $x(u,t)$  is the generated series.
- $h_j(u)$  is the  $j$ 'th weight coefficient for series at location  $u$ .
- $\beta_j(t)$  is the  $j$ 'th amplitude function.
- $s(u)$  is the standard deviation of the series.
- $m(u)$  is the mean value.
- $k$  is the first weight coefficient and amplitude function to be used.
- $n$  is the last weight coefficient and amplitude function to be used.

E.g., if only the first component is used,  $k=n=1$ .

Only  $9\sigma$ -filtered series were analysed. The locations of the stations used are indicated in figure 5.1.

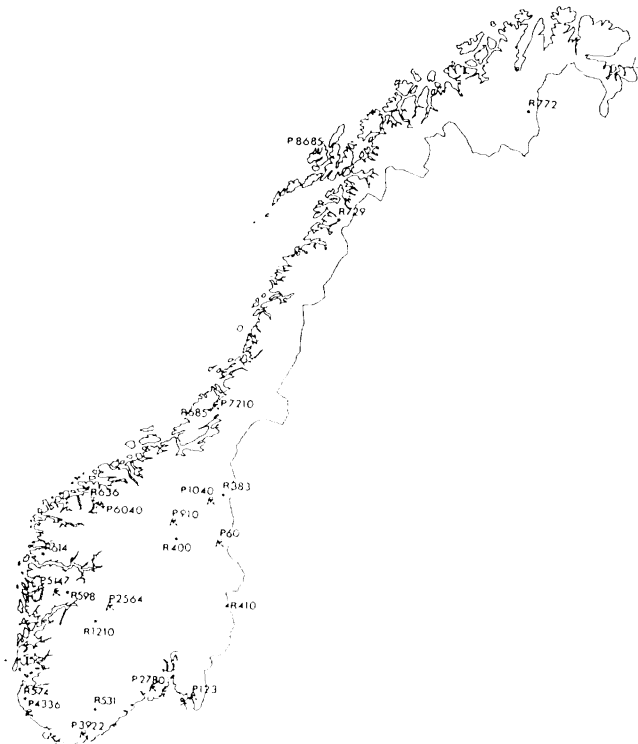


Figure 5.1 Locations of the test series.

The regional estimates were calculated for 12 runoff and 12 precipitation series selected from all over Norway. In figure 5.2 hydrographs and hyetographs from each of the regions marked in figure 4.4 are plotted. In table 5.1 the variance contribution from the individual amplitude functions in the selected series are shown. The runoff and precipitation series in figure 5.2 and table 5.1 are selected as typical for their regions.

Table 5.1 Explained variances by the first three amplitude functions for runoff and precipitation at selected stations.

Region	Type/Station	1. amp.f.	2. amp.f.	3. amp.f.
1	Runoff-410	3%	60%	26%
	Prec.-910	0%	50%	35%
2	Runoff-574	97%	1%	1%
	Prec.-4336	99%	0%	0%
3	Runoff-614	98%	1%	0%
	Prec.-5147	96%	1%	0%
4	Runoff-636	77%	15%	1%
	Prec.-7210	80%	14%	3%
5	Runoff -729	77%	13%	9%
	Prec.-8685	63%	30%	6%

The results show that the variance coverage in runoff and precipitation coincides in all regions. In region 1 the second amplitude function dominates. The third function also gives a significant contribution. The second function represents south-easterly/north-westerly weather systems. Region 2 and 3 are totally dominated by the first function, representing westerly weather types. Region 4, at the northwest coast and Trøndelag, and region 5 are dominated by the first function, but the second function also contributes.

The study verifies that the different functions contain information about variability in runoff and precipitation due to different dominating wind directions or climate types. The first function containing the southwesterly to westerly winds, and the second function containing winds around the northwest/southeast axis. The third function is more difficult to interpret, but it seems to cover variations in the inland zone, caused by convective activity. These results coincide with the knowledge of different weather systems dominating in different parts of the country.

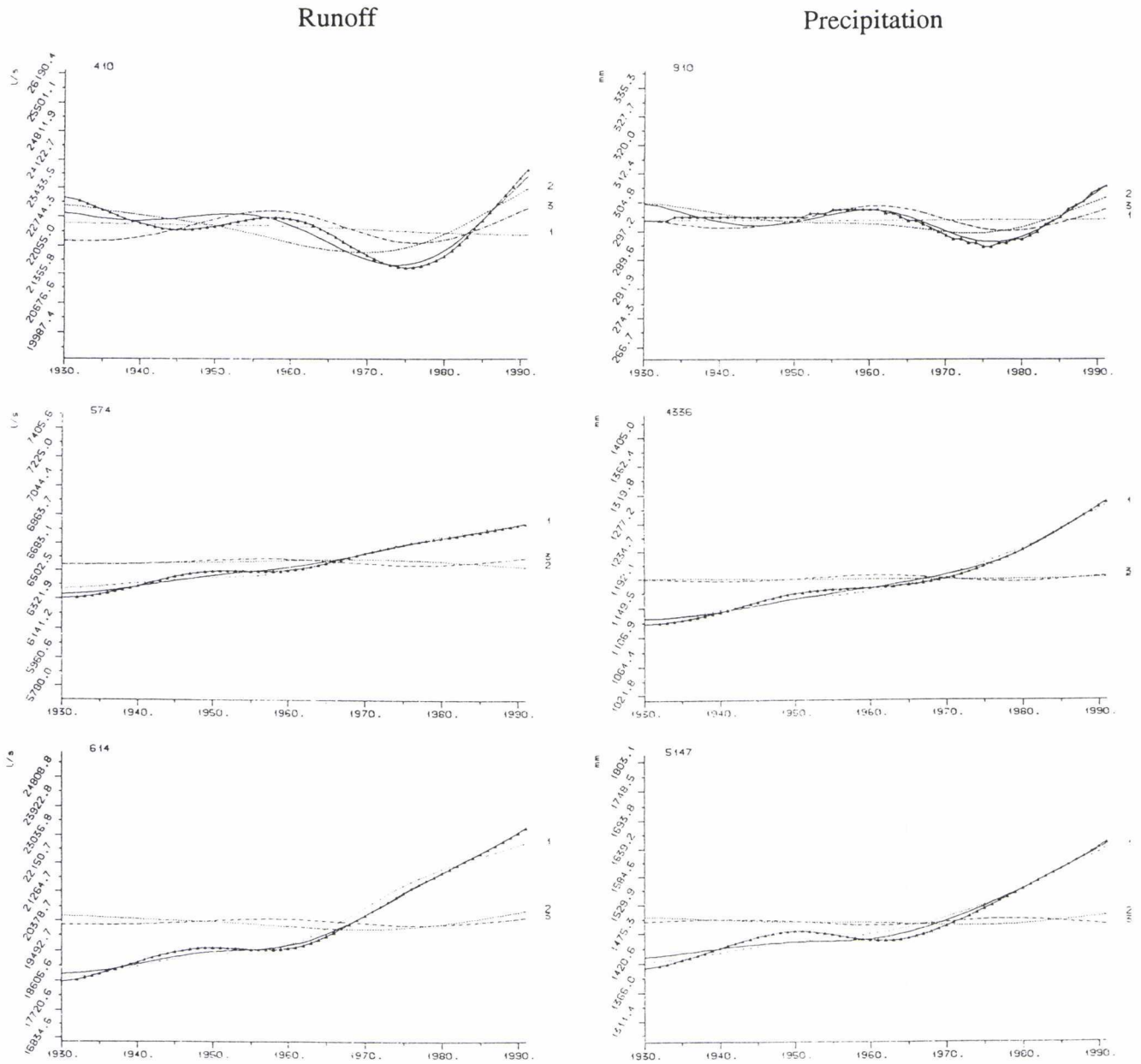


Figure 5.2 Hydrographs and hyetographs for the selected series. The observed series is plotted as a solid line, the first amplitude function contribution as a dotted line, the second amplitude function contribution as a dashed line and the third amplitude function contribution as a dash-dotted line. The resulting series of all three functions is plotted as a solid line with  $\Delta$  markers.

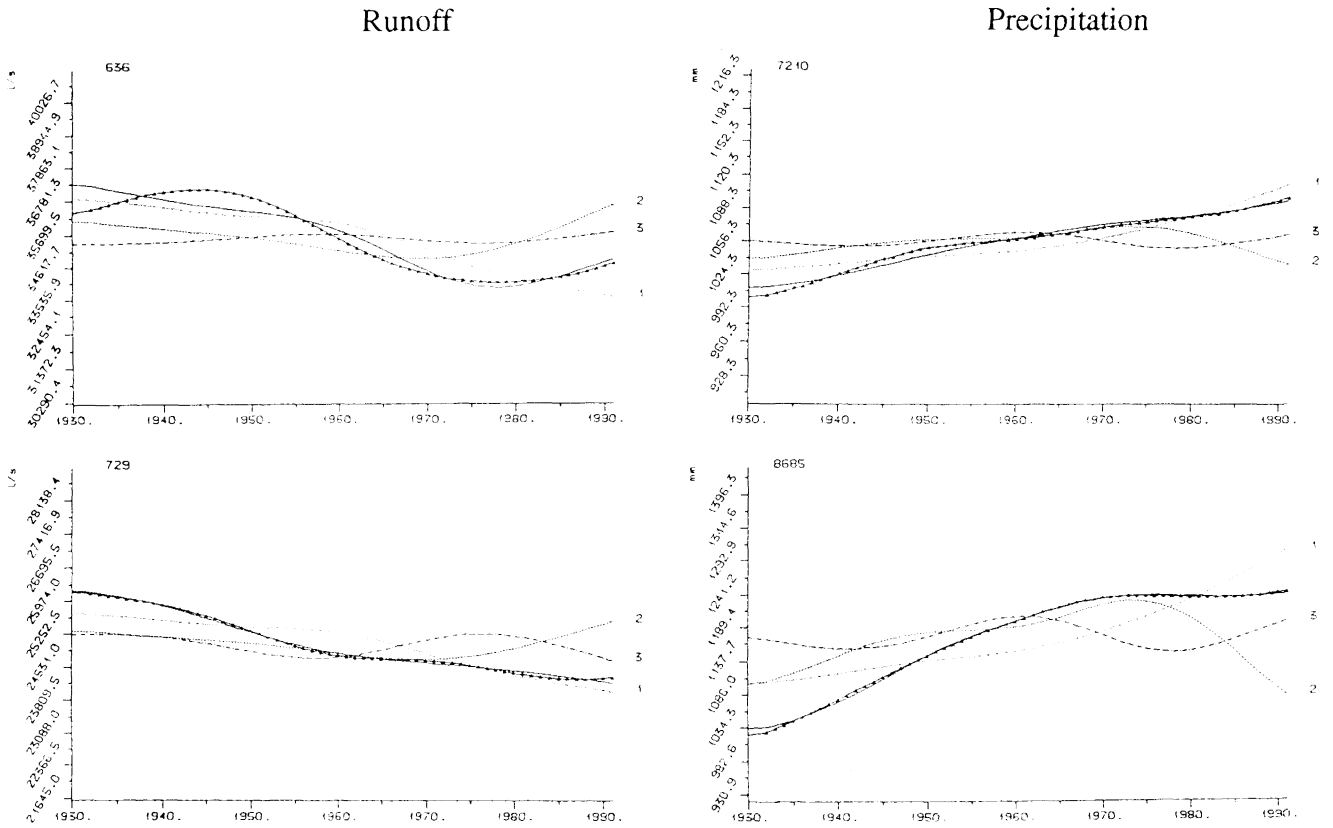


Figure 5.2 Continued.

## **6 CONCLUSIONS**

The EOF-method has been used for identification of trends and regional patterns in homogenous runoff and precipitation series. The number of significant amplitude functions explaining the variation in time, is three to five. In this study the first three functions are examined. They cover 71 to 93% of the original variance. The lower ranked functions may also contribute to the variance. In most cases this information can be regarded as noise.

The study shows that the temporal variation of runoff and precipitation coincide. An optimal cover of data for climatic analysis may therefore be obtained by using a combination of these variables. The result is important for extrapolation purposes in future research.

Annual values of runoff and rainfall amplitude functions have the same properties. The deviations occurring in the analysis of seasonal values are caused by storage effects (snow/glacier cover) and the difference between point and catchment processes.

Trends can be detected studying filtered series, especially when the  $9\sigma$  filter is used. In the first amplitude function periods close to a thirty-year interval appear. Analysing the three periods 1900-30, 1930-60 and 1960-90, the results from the first and last period are different from that of the second period. This is caused by a variation of the main weather type which is explained by the first and second amplitude function. Amplitude functions based on annual unfiltered series cannot be used to identify trends.

Regional verifications show that the different characteristics of the amplitude functions can be explained by dominating weather types. Different amplitude functions explain the main part of the variation in runoff and precipitation in different parts of the country. This is confirmed by considering these geographical areas and the extent to which they are exposed to different weather systems. This is in accordance with the results of the studies of the contour plots and scatterplots

To get a better understanding of the physical properties of the amplitude functions, studies are required to find relations between other large scale phenomena and the runoff/precipitation components. This is necessary when evaluating the local influence of output from climatic models as well.

## REFERENCES

- Aagenæs,K.H. (1993)  
*Hydrologiske Data - Homogenitetstest*, NVE HD-notat 1-1993, Oslo
- Essenwanger, (1976)  
*Applied statistics in Atmospheric Science*, Development in Atmospheric Science, Elsevier, Amsterdam
- Førland,E. , Hanssen-Bauer,I. and Nordli,P.Ø. (1991)  
*Langtidsvariasjoner av nedbør (Long time variations in precipitation; In Norwegian)*, DNMI-klima rapport 02/91, Det Norske Meteorologiske Institutt, Oslo
- Førland,E. and Hanssen-Bauer,I (1992)  
*Analyse av lange nedbørserier (Analysis of long precipitation series; In Norwegian)*, DNMI-klima rapport 01/92, Det Norske Meteorologiske Institutt, Oslo
- Hisdal,H and Tveito,O.E. (1990)  
*Regioninndeling med henblikk på EOF-metoden (Regionalization with a view to the EOF-method; In Norwegian)*, NVE Oppdragsrapport 4-90, Oslo
- Hisdal,H and Tveito,O.E. (1992)  
*Generation of runoff series at ungauged locations using empirical orthogonal functions in combination with kriging*, Stochastic Hydrology and Hydraulics, 6, 4, pp 255-269
- Hisdal,H and Tveito,O.E. (1993)  
*Extension of runoff series by the use of empirical orthogonal functions*, Hydrological Sciences Journal 38, 1, 2, pp 33-49
- Lins,H.F. (1985)  
*Interannual streamflow variability in the United States based on principal components*, Water Resources Research, 21, 5, pp 691-701
- Pandžić,K and Trninić,D. (1991)  
*Principal component analysis of the annual regime og hydrological and meteorological fields in a river basin*, International Journal of Climatology, 11, pp 909-922
- Preissendorfer, (1988)  
*Principal component analysis in Meteorolgy and Oceanography*, Elsevier, Amsterdam
- Roald,L and Sælthun,N.R. (1990)  
*Langtidsvariasjoner av avløpet i Norge (Long time variations in runoff in Norway; in Norwegian)*, Paper presented at Nordic Hydrological Conference, Kalmar, Sweden.



Denne serien utgis av Norges vassdrags- og energiverk (NVE)  
Adresse: Postboks 5091 Majorstua, 0301 Oslo

#### **I 1994 ER FØLGENDE RAPPORTER UTGITT:**

- Nr 1 Truls Erik Bønsnes og Lars Andreas Roald: Regional flomfrekvensanalyse. Sambandet mellom momentanflom og døgnmiddelflom. (45 s.)
- Nr 2 Steinar Myrabø: Sæternbekken forsøksfelt. (29 s.)
- Nr 3 Edward Witczak: Vurdering av grustak i Stjørdalselva ved Måsøra - Hofstadøra. Stjørdal kommune, N-Trøndelag. Vassdrag nr. 124. A0. (11 s.)
- Nr 4 Bjarne Krokli: Q 100 og Q 1000 avløpsflom med naturlig utløpsprofil i Ulldalsvatn og Bergsvatn (079.Z). (13 s.)
- Nr 5 Rune Dahl, Hans Otnes og Frode Trengereid: Årsrapport for NVEs interne havarigruppe. (8 s.)
- Nr 6 Harald Sakshaug: Vassdragsteknisk vurdering av interimsvai ved bygging av ny Vikersund bru. (5 s.)
- Nr 7 Astrid Voksø, Bjarne Krokli: Flomlinjeberegning og flomsonekart for nedre del av Leira (002. CAZ). (9 s.)
- Nr 8 Lars-Evan Pettersson: Flomberegning Lærdalsvassdraget (073.Z). (36 s.)
- Nr 9 Ole Einar Tveito og Hege Hisdal: A study of regional trends in annual and seasonal precipitation and runoff series. (30 s.)